Procedure for obtaining microscopic mechanisms of reconstructive phase transitions in crystalline solids

Harold T. Stokes and Dorian M. Hatch
Department of Physics and Astronomy, Brigham Young University, Provo, Utah 84602
(Received 17 November 2001; published 4 April 2002)

A procedure for obtaining possible microscopic mechanisms for reconstructive phase transitions in crystalline solids is described. Both strains and atomic displacements are considered, and the procedure includes user input of allowed strain tolerance, nearest-neighbor distances, and unit-cell size change. This method has been implemented in a computer program COMSUBS. We apply COMSUBS to the pressure-induced phase transition in NaCl and obtain 12 possible mechanisms, two of which are those proposed earlier by Buerger and Watanabe, respectively. Furthermore, we show how to use energy calculations to determine the height of the energy barrier for the transition.

DOI: 10.1103/PhysRevB.65.144114 PACS number(s): 64.70.Kb, 02.20.−a, 71.15.Nc

I. INTRODUCTION

In a reconstructive phase transition, there is no group-subgroup relation between the symmetries of the two crystalline phases. The path from one phase to the other phase requires significant strain and/or large atomic displacements.

Examples of reconstructive phase transitions abound in nature. Many of the alkali halides undergo a transition from a NaCl-type structure to a CsCl-type structure. Motivated by the use of these solids, and in particular the use of NaCl as a pressure standard, this transition type has been studied with considerable effort.[1–6] Many alkali metals and transition metals undergo a transition from the hcp to bcc phase.[7] Ti, representative of the transition metals, undergoes a transition from the α to the ω phase. This transition was first observed by Jamieson[8] and has been studied extensively since then with static high-pressure[9–11] and shock-wave techniques.[12] The wurtzite to rocksalt transition in GaN,[13] the bcc to fcc transition in Cs,[14] the fcc to hcp transition in Co, Fe, Tl, and Am,[15] the bcc to rutile type transition of SiO_2,[16] and many other examples that could be mentioned stress the importance and interest in this kind of phase transformation.

Any detailed description of a reconstructive phase transition must deal with two questions: (1) How are the atoms mapped from one structure to the other? (2) What path do the atoms take between these two structures? The mapping question simply deals with how the two structures are related. The path question is more difficult. It deals with actual atomic displacements and strains that occur during the phase transition. In a previous paper we presented a systematic procedure for obtaining possible mappings and paths for a reconstructive phase transition[17] based almost entirely on symmetry considerations. In this paper we generalize that algorithmic procedure by considering a wider class of subgroups, by allowing user input for some important parameters (allowed strain, nearest-neighbor distances, and unit-cell size change) and by implementing the procedure on computer.

In our treatment, we assume that the path between the two structures involves an intermediate unstable structure with definite space-group symmetry G. If we are considering a reconstructive phase transition from a structure with space-group symmetry G_1 to a structure with space-group symmetry G_2, then our description is actually a two-step process $G_1 \rightarrow G \rightarrow G_2$, where G is a subgroup of G_1 and also a subgroup of G_2 so that each step $G_1 \rightarrow G$ and $G \rightarrow G_2$ is a transition with a group-subgroup relationship.

Therefore, our approach is based on a search for common subgroups of G_1 and G_2. For a given common subgroup G, we then consider possible mappings of atoms from G_1 to G_2. The mappings are restricted by the constraint that the symmetry G must be maintained along the entire path from G_1 to G_2. No atomic displacements are allowed which destroy the symmetry G.

As an example, we apply our procedure to the pressure-induced phase transition in NaCl. At ambient pressure, NaCl exists in the well-known face-centered-cubic (fcc) structure with space-group symmetry $Fm\bar{3}m$. When the pressure is raised to $\approx$30 GPa, NaCl changes to a CsCl-like simple cubic (sc) structure with space-group symmetry $Pm\bar{3}m$. This pressure-induced transition has physical and geological importance as it can be a basic model of other solid-solid transitions due to its simplicity. The transition has been heavily studied but still, today, remains an interesting example for investigation, particularly when new methods of experimental investigation can be applied and new schemes of model calculations used.

Over the years, two main models have been proposed for this phase transition. The first one was proposed by Shoji[18] and later modified by Buerger.[2] Buerger showed that a contraction along one of the body diagonals of the unit cell of the NaCl structure and an expansion normal to it lead to the CsCl structure. In this model the transition is accomplished via strains alone. Another model was introduced by Hyde and O'Keefe[19] and emphasized later by Watanabe *et al.*[6] In this model the orientation relation is not the same as in the Buerger model; instead the $[110]_{CsCl}$ is parallel to $[100]_{NaCl}$, and $[001]_{CsCl}$ is parallel to $[011]_{NaCl}$. They describe the transition as an interplanar movement and a shuffle of atoms in adjacent $(100)_{NaCl}$ planes in an antiparallel manner.

We have implemented our method as a computer program called COMSUBS. When applied to the case of the phase transition in NaCl, COMSUBS finds 12 possible paths, 2 of which

are the Buerger and Watanabe mechanisms mentioned above.

We carry the example further by using energy calculations to find the barrier heights for the various paths found. In the case of the Buerger mechanism, we refine the path Buerger proposed and show that the energy barrier can be significantly lowered by including additional strains and atomic displacements.

II. COMSUBS ALGORITHM

Consider two crystalline structures with space-group symmetries G_1 and G_2, respectively. We are given the lattice parameters which define the size and shape of the unit cell, and we are given the positions of atoms inside the unit cell. Space-group operators are denoted using the Seitz notation $\{\hat{R}|\vec{v}\}$, i.e., a point operation $\hat{R}$ followed by a translation $\vec{v}$ of the crystal. For space group G_i, we designate a set of representative operators $\{\hat{R}_{ij}|\vec{v}_{ij}\}$, one for each point operation $\hat{R}_{ij}$.

The set of all pure translations in a space group forms its translation group. In three dimensions, translation groups can be generated with three primitive translations. We define the translation $\vec{t}_{ik}$ to be the kth generator of the translation group T_i associated with G_i. The action of a point operation $\hat{R}_{ij}$ on the generator $\vec{t}_{ik}$ results in a linear combination of the three generators,

$$\hat{R}_{ij}\vec{t}_{ik}=\sum_m (\hat{R}_{ij})_{mk}\vec{t}_{im}, \tag{1}$$

where the matrix elements $(\hat{R}_{ij})_{mk}$ are all integers since every point operation in a space group takes the lattice into itself.

Our goal is to find possible paths from G_1 to G_2 such that the strains and atomic displacements that occur along these paths do not exceed some chosen reasonable limits. We allow all possible relative orientations and origins of G_1 and G_2. We assume that along the path from G_1 to G_2, the space-group symmetry of the crystal is some common subgroup of G_1 and G_2. Thus, to accomplish our goal, we search for common symmetry subgroups.

We begin by searching for common sublattices, i.e., common subgroups T of the translation groups T_1 and T_2. We write the generators $\vec{s}_{ij}$ of T in terms of the generators of T_1 and the generators of T_2,

$$\vec{s}_{ij}=\sum_k (A_i)_{kj}\vec{t}_{ik}, \tag{2}$$

where the matrix elements $(A_i)_{kj}$ are all integers.

Along the path from T_1 to T_2, the generators of T evolve from $\vec{s}_{1j}$ to $\vec{s}_{2j}$. From the two end points of this path, $\vec{s}_{1j}$ and $\vec{s}_{2j}$, we can determine the minimum total strain required to go from T_1 to T_2. We use the method of magic strains.[20] We first write the generators of T in terms of Cartesian coordinates:

$$\vec{s}_{ij}=\sum_k (B_i)_{kj}\hat{e}_k, \tag{3}$$

where $\hat{e}_1,\hat{e}_2,\hat{e}_3$ are unit vectors along Cartesian x,y,z axes, respectively. If we define a transformation matrix S by $B_2=SB_1$, the principal values of the strain tensor are given by the square root of the eigenvalues of S^TS, where S^T is the transpose of S. The product S^TS removes any antisymmetric part of S due to pure rotations which may be introduced by the arbitrary choice of relative coordinate systems for T_1 and T_2.

Now we can test whether or not the strain exceeds some reasonable limit. We require that each principal value of the strain tensor be less than $1+\epsilon$ and greater than $(1+\epsilon)^{-1}$, where ϵ is a parameter which we usually choose to be 0.50. This rather liberal constraint results in a large number of possible common sublattices to be investigated further.

As an example, consider the pressure-induced phase transition in NaCl. For the low-pressure structure, $G_1=Fm\bar{3}m$ with lattice parameter $a_1=4.84$ Å. For the high-pressure structure, $G_2=Pm\bar{3}m$ with lattice parameter $a_2=2.98$ Å. In terms of Cartesian coordinates, the generators of T_1 and T_2 are

$$\begin{aligned}
\vec{t}_{11}&=(0,\tfrac{1}{2}a_1,\tfrac{1}{2}a_1),\\
\vec{t}_{12}&=(\tfrac{1}{2}a_1,0,\tfrac{1}{2}a_1),\\
\vec{t}_{13}&=(\tfrac{1}{2}a_1,\tfrac{1}{2}a_1,0),\\
\vec{t}_{21}&=(a_2,0,0),\\
\vec{t}_{22}&=(0,a_2,0),\\
\vec{t}_{23}&=(0,0,a_2).
\end{aligned} \tag{4}$$

We limit the scope of our search by specifying a maximum allowed length for any of the generators $\vec{s}_{ij}$ of T. In NaCl, we consider only generators of length 6 Å or less. This results in a list of 42 possible vectors $\vec{s}_{1j}$ for G_1 and 32 vectors $\vec{s}_{2j}$ for G_2. This effectively limits the size of the unit cell of T. If we wanted to consider larger unit cells, then we would need to allow longer generators $\vec{s}_{ij}$.

We next consider all possible triplets of generators $\vec{s}_{1j}$ of T. Given 42 possible generators, this would result in 11 480 triplets. We limit this number by requiring that $\det A_1>0$. We further require that as each triplet is considered, it represent a different set of lattice points than any previously considered triplet. Two sets of generators with matrices A_1 and A_1' represent different lattices if either $|\det A_1|\neq|\det A_1'|$ or $A_1^{-1}\hat{R}_{1j}A_1'$ contains any noninteger elements for any point operator $\hat{R}_{1j}$ in G_1. For NaCl, this results in only ten triplets of generators $\vec{s}_{1j}$ of T to be considered further.

Next, given a triplet of generators $\vec{s}_{1j}$, we consider all possible triplets of generators $\vec{s}_{2j}$ such that

$$(1+\epsilon)^{-1}<s_{2j}/s_{1j}<1+\epsilon \tag{5}$$

for each of the three pairs of generators $\vec{s}_{1j},\vec{s}_{2j}$. We further test the two triplets by calculating the principal values of the

strain tensor and require that they also lie between the values of $(1+\epsilon)^{-1}$ and $1+\epsilon$. This guarantees that not only the lengths of $\vec{s}_{1j}$ and $\vec{s}_{2j}$ agree (to within the accuracy specified by ϵ), but also the angles between the pairs $\vec{s}_{1j},\vec{s}_{1j'}$ and $\vec{s}_{2j},\vec{s}_{2j'}$ also agree. Last, we require that $\det A_2>0$ and that the unit cells specified by the generators $\vec{s}_{1j}$ and by the generators $\vec{s}_{2j}$ contain the same number of atoms. If the primitive unit cell of G_i contains N_i atoms, then this means that $N_1 \det A_1 = N_2 \det A_2$. For NaCl, using $\epsilon=0.5$, this results in a total of 343 matched sets of lattices, each of which we consider further as a possible path for the phase transition.

Let us pursue this example further by considering a particular pair of matched lattices: a subgroup of T_1 generated by

$$\vec{s}_{11}=-\vec{t}_{11}=(0,-\tfrac{1}{2}a_1,-\tfrac{1}{2}a_1),$$

$$\vec{s}_{12}=-\vec{t}_{11}-\vec{t}_{12}+\vec{t}_{13}=(0,0,-a_1),$$

$$\vec{s}_{13}=-\vec{t}_{11}+\vec{t}_{12}+\vec{t}_{13}=(a_1,0,0), \tag{6}$$

i.e.,

$$A_1=\begin{pmatrix} -1 & -1 & -1 \\ 0 & -1 & 1 \\ 0 & 1 & 1 \end{pmatrix} \tag{7}$$

and

$$B_1=a_1\begin{pmatrix} 0 & 0 & 1 \\ -1/2 & 0 & 0 \\ -1/2 & -1 & 0 \end{pmatrix}, \tag{8}$$

and a subgroup of T_2 generated by

$$\vec{s}_{21}=\vec{t}_{22}=(0,a_2,0),$$

$$\vec{s}_{22}=\vec{t}_{21}+\vec{t}_{22}+\vec{t}_{23}=(a_2,a_2,a_2),$$

$$\vec{s}_{23}=\vec{t}_{21}-\vec{t}_{23}=(a_1,0,-a_1), \tag{9}$$

i.e.,

$$A_2=\begin{pmatrix} 0 & 1 & 1 \\ 1 & 1 & 0 \\ 0 & 1 & -1 \end{pmatrix} \tag{10}$$

and

$$B_2=a_2\begin{pmatrix} 0 & 1 & 1 \\ 1 & 1 & 0 \\ 0 & 1 & -1 \end{pmatrix}. \tag{11}$$

A continuous evolution from the subgroup of T_1 to the subgroup of T_2 would define a possible path for the phase transition. We can see that such a path would require a strain in the lattice. For example, the lengths of $\vec{s}_{1j}$ and $\vec{s}_{2j}$ are different. Also, the angle between $\vec{s}_{i1}$ and $\vec{s}_{i2}$ changes from 45° to 54.7°. Using the method of magic strains, we can find the principal values of the strain tensor. From the matrices, B_1 and B_2, we obtain

$$S=B_2B_1^{-1}=\frac{a_2}{a_1}\begin{pmatrix} 1 & 1 & -1 \\ 0 & -1 & -1 \\ -1 & 1 & -1 \end{pmatrix}. \tag{12}$$

The square roots of the eigenvalues of S^TS are 1.23, 0.87, 0.87, which are therefore the principal values of the strain tensor. We can see that each of these values is greater than $(1+\epsilon)^{-1}=0.66$ and less than $1+\epsilon=1.5$ (using $\epsilon=0.5$). Using this criterion, the path between these two lattices is acceptable for further consideration.

Using one of the common sublattices T of T_1 and T_2, we can next construct space groups G which are common subgroups of G_1 and G_2. First we find the point group P of T. This is the intersection of P_1 and P_2, where P_i is the set of point operations $\hat{R}_{ij}$ in G_i which are also point operations of T at the end point of the path where $G\rightarrow G_i$. Consider the action of a point operator $\hat{R}_{ij}$ on one of the generators $\vec{s}_{ik}$ of T_i. We have

$$\begin{aligned}\hat{R}_{ij}\vec{s}_{ik}&=\sum_m (A_i)_{mk}\hat{R}_{ij}\vec{t}_{im}\\ &=\sum_{m,n}(A_i)_{mk}(\hat{R}_{ij})_{nm}\vec{t}_{in}\\ &=\sum_{m,n,p}(A_i)_{mk}(\hat{R}_{ij})_{nm}(A_i^{-1})_{pn}\vec{s}_{ip}\\ &=\sum_p (A_i^{-1}\hat{R}_{ij}A_i)_{pk}\vec{s}_{ip}.\end{aligned} \tag{13}$$

We see that if $\hat{R}_{ij}\in P_i$, then every element of the matrix $A_i^{-1}\hat{R}_{ij}A_i$ must be an integer. Using this test, we can find every operator in P_1 and in P_2. The intersection of P_1 and P_2 requires that

$$A_1^{-1}\hat{R}_{1j}A_1=A_2^{-1}\hat{R}_{2j'}A_2 \tag{14}$$

for pairs of point operations $\hat{R}_{1j}$ and $\hat{R}_{2j'}$ in G_1 and G_2, respectively. The equality in the above equation means that the two matrices are equal, element by element. The above equation also defines a mapping of point operations $\hat{R}_{1j}$ in G_1 onto point operations $\hat{R}_{2j'}$ in G_2. Along the path from G_1 to G_2, each point operation $\hat{R}_{1j}$ at the beginning of the path evolves into the point operation $\hat{R}_{2j'}$ at the end of the path. For convenience, we renumber the point operations in G_2 so that $j'=j$.

Let us consider the above example further. For the point operator C_{2x} (180° rotation about the x axis, using the notation of Miller and Love[21]), we have

$$\hat{R}_1(C_{2x})=\begin{pmatrix} -1 & -1 & -1 \\ 0 & 0 & 1 \\ 0 & 1 & 0 \end{pmatrix} \tag{15}$$

and

$$A_1^{-1}\hat{R}_1(C_{2x})A_1=\begin{pmatrix}-1&0&0\\0&-1&0\\0&0&1\end{pmatrix}, \tag{16}$$

which contains all integers. Therefore $C_{2x}\in P_1$. Similarly,

$$\hat{R}_1(C_{2y})=\begin{pmatrix}0&0&1\\-1&-1&-1\\1&0&0\end{pmatrix} \tag{17}$$

and

$$A_1^{-1}\hat{R}_1(C_{2y})A_1=\begin{pmatrix}1&0&0\\-1&-1&0\\0&0&-1\end{pmatrix}, \tag{18}$$

and we see that $C_{2y}\in P_1$. On the other hand, for C_{4z}^{+} (90° rotation about the z axis) we have

$$\hat{R}_1(C_{4z}^{+})=\begin{pmatrix}1&1&1\\0&0&-1\\-1&0&0\end{pmatrix} \tag{19}$$

and

$$A_1^{-1}\hat{R}_1(C_{4z}^{+})A_1=\begin{pmatrix}0&0&-2\\1/2&1&1\\1/2&0&0\end{pmatrix}, \tag{20}$$

and we see that $C_{4z}^{+}\notin P_1$. Repeating this process for each of the 48 point operators in G_1, we find that $P_1=4/mmm$ with the fourfold axis pointing along the x axis.

To find P, we see from Eq. (14) that $\hat{R}_{2j'}=A_2A_1^{-1}\hat{R}_{1j}A_1A_2^{-1}$, and we therefore calculate $A_2A_1^{-1}\hat{R}_{1j}A_1A_2^{-1}$ for each operator $\hat{R}_{1j}$ in P_1 and check if the result is a point operator in G_2. For example,

$$A_2A_1^{-1}\hat{R}_1(C_{2x})A_1A_2^{-1}=\begin{pmatrix}0&0&-1\\0&-1&0\\-1&0&0\end{pmatrix}, \tag{21}$$

which is the point operator C_{2e} in G_2 (180° rotation about $\hat{\mathbf{i}}-\hat{\mathbf{k}}$) and therefore $C_{2x}\in P$. On the other hand,

$$A_2A_1^{-1}\hat{R}_1(C_{2y})A_1A_2^{-1}=\begin{pmatrix}1/2&-1&1/2\\-1/2&0&-1/2\\1/2&-1&-1/2\end{pmatrix}, \tag{22}$$

and $C_{2y}\notin P$. Applying this test to each of the 16 operators in P_1, we obtain $P=mmm$ with the twofold axes along $\hat{\mathbf{i}}$, $\hat{\mathbf{j}}-\hat{\mathbf{k}}$, $\hat{\mathbf{j}}+\hat{\mathbf{k}}$ in G_1 and along $\hat{\mathbf{i}}-\hat{\mathbf{k}}$, $\hat{\mathbf{i}}+\hat{\mathbf{k}}$, $\hat{\mathbf{j}}$ in G_2.

The point group of G will be some subgroup of the lattice point group P. Therefore, consider some point group $P'\subset P$. The representative operators of G will be of the form $\{\hat{R}_j|\vec{v}_j\}$, where $\hat{R}_j\in P'$ and is equal to $\hat{R}_{1j}$ in G_1 and equal to $\hat{R}_{2j}$ in G_2. The operator $\{\hat{R}_j|\vec{v}_j\}$ in G must be identical to some operator $\{R_{1j}|\vec{v}_{1j}+\vec{u}_{1j}\}$ in G_1 and also to some operator $\{R_{2j}|\vec{v}_{2j}+\vec{u}_{2j}\}$ in G_2, where $\vec{u}_{1j}\in T_1$ and $\vec{u}_{2j}\in T_2$. If we also include a possible shift $\vec{\tau}$ in the origin of G_2 with respect to G_1, we obtain the requirement

$$\vec{v}_j=\vec{v}_{1j}+\vec{u}_{1j}=\vec{v}_{2j}+\vec{u}_{2j}+\hat{R}_{2j}\vec{\tau}-\vec{\tau}. \tag{23}$$

In practice, we write each vector in this equation in terms of the generators $\vec{s}_{ik}$ of T_i. Consider a vector $\vec{v}_{ij}$ written in terms of the generators $\vec{t}_{ik}$ of T_i:

$$\vec{v}_{ij}=\sum_k C_k\vec{t}_{ik}. \tag{24}$$

Using the appropriate transformation, we can express this vector in terms of the generators $\vec{s}_{im}$ of T:

$$\vec{v}_{ij}=\sum_{k,m} C_k(A_i^{-1})_{mk}\vec{s}_{im}=\sum_m (A_i^{-1}C)_m\vec{s}_{im}. \tag{25}$$

We will simply denote this by the shorthand notation $A_i^{-1}\vec{v}_{ij}$, which means a multiplication of the matrix A_i^{-1} and the column matrix $\vec{v}_{ij}$ where the three rows contain the components of $\vec{v}_{ij}$ in terms of the generators of T_i. The result is a column matrix containing the components of $\vec{v}_{ij}$ in terms of the generators of T. Using this notation, we write the requirement in Eq. (23) more precisely as

$$\vec{v}_j=A_1^{-1}(\vec{v}_{1j}+\vec{u}_{1j})=A_2^{-1}(\vec{v}_{2j}+\vec{u}_{2j}+\hat{R}_{2j}\vec{\tau}-\vec{\tau}). \tag{26}$$

We must find vectors $\vec{u}_{1j}$, $\vec{u}_{2j}$, and $\vec{\tau}$ which satisfy simultaneously Eq. (26) for each operator $\hat{R}_j\in P'$. In practice, we need only consider the operators corresponding to the generators of P'. If there are N generators, then we must find a value of $\vec{\tau}$ and values of the N pairs of vectors, $\vec{u}_{1j}$ and $\vec{u}_{2j}$, which satisfy simultaneously N equations.

We proceed as follows. We try every possible value of $\vec{u}_{1j}$ in each of the N equations. The value of $\vec{u}_{1j}$ can be restricted to the translations in T_1 which are inside the primitive unit cell of T (including $\vec{u}_{1j}=0$). For each set of these N $\vec{u}_{1j}$ values, we try to solve the N equations simultaneously for $\vec{\tau}$ and the vectors $\vec{u}_{2j}$ using the method of Smith normal forms.[22] If successful, we can use the resulting generators $\{\hat{R}_j|\vec{v}_j\}$ to obtain the remaining operators in G. One more requirement must then be satisfied. The operators in G must obey group multiplication. For every pair of point operations $\hat{R}_j\hat{R}_k=\hat{R}_m$, we must require that

$$\vec{v}_j+\hat{R}_j\vec{v}_k=\vec{v}_m \tag{27}$$

to within a lattice vector in T. Having passed this final requirement, we now have a space group G which is a subgroup of both G_1 and G_2.

Consider again the above example. A set of generators of P are C_{2x},C_{2f},I in P_1 and C_{2e},C_{2c},I in P_2. Since $\det A_1=2$, there are two vectors $\vec{u}_{1j}$ to be considered: namely, $\vec{u}_{1j}=0$ and $\vec{u}_{1j}=-\vec{t}_{11}+\vec{t}_{13}=a_1(\frac{1}{2},0,-\frac{1}{2})$. There are eight

ways of assigning u_{1j} to the three generators of P. Only two of them result in a solution to the three equations (26).

(1) $\vec{u}_{11}=\vec{u}_{12}=\vec{u}_{13}=0$. This results in $\vec{v}_1=\vec{v}_2=\vec{v}_3=0$, and the three equations (26) can be satisfied with $\vec{\tau}=0$ and $\vec{u}_{21}=\vec{u}_{22}=\vec{u}_{23}=0$. In other words, the generating elements of G are $\{C_{2x}|0\},\{C_{2f}|0\},\{I|0\}$ when $G\rightarrow G_1$ and $\{C_{2e}|0\},\{C_{2c}|0\},\{I|0\}$ when $G\rightarrow G_2$. Using an algorithm of Hatch and Stokes,[23] we identify the space group $G=Pmmm$ with the three principal lattice vectors

$$\vec{s}'_{11}=-\vec{t}_{11}+\vec{t}_{12}+\vec{t}_{13}=a_1(1,0,0),$$

$$\vec{s}'_{12}=-\vec{t}_{11}=a_1(0,-\tfrac{1}{2},-\tfrac{1}{2}),$$

$$\vec{s}'_{13}=-\vec{t}_{12}+\vec{t}_{13}=a_1(0,\tfrac{1}{2},-\tfrac{1}{2}),$$

$$\vec{s}'_{21}=\vec{t}_{21}-\vec{t}_{23}=a_2(1,0,-1),$$

$$\vec{s}'_{22}=\vec{t}_{22}=a_2(0,1,0),$$

$$\vec{s}'_{23}=\vec{t}_{21}+\vec{t}_{23}=a_2(1,0,1). \tag{28}$$

These are simply a rearrangement of the generators $\vec{s}_{ij}$ of T and define the $\vec{a},\vec{b},\vec{c}$ axes of G.

(2) $\vec{u}_{11}=\vec{u}_{12}=\vec{u}_{13}=-\vec{t}_{11}+\vec{t}_{13}$. This results in $\vec{v}_1=\vec{v}_2=\vec{v}_3=\frac{1}{2}\vec{s}_{12}+\frac{1}{2}\vec{s}_{13}$ and the three equations can be satisfied with $\vec{\tau}=-\frac{1}{4}\vec{t}_{22}$ and $\vec{u}_{21}=\vec{u}_{22}=\vec{u}_{23}=\vec{t}_{21}$. In other words, the generating elements of G are $\{C_{2x}|-\vec{t}_{11}+\vec{t}_{13}\}$, $\{C_{2f}|-\vec{t}_{11}+\vec{t}_{13}\}$, $\{I|-\vec{t}_{11}+\vec{t}_{13}\}$ when $G\rightarrow G_1$ and $\{C_{2e}|\vec{t}_{21}+\frac{1}{2}\vec{t}_{22}\}$, $\{C_{2c}|\vec{t}_{21}+\frac{1}{2}\vec{t}_{22}\}$, $\{I|\vec{t}_{21}+\frac{1}{2}\vec{t}_{22}\}$ when $G\rightarrow G_2$. We identify the space group $G=Pmmn$ with the three principal lattice vectors

$$\vec{s}'_{11}=-\vec{t}_{11}+\vec{t}_{12}+\vec{t}_{13}=a_1(1,0,0),$$

$$\vec{s}'_{12}=-\vec{t}_{12}+\vec{t}_{13}=a_1(0,\tfrac{1}{2},-\tfrac{1}{2}),$$

$$\vec{s}'_{13}=\vec{t}_{11}=a_1(0,\tfrac{1}{2},\tfrac{1}{2}),$$

$$\vec{s}'_{21}=\vec{t}_{21}-\vec{t}_{23}=a_2(1,0,-1),$$

$$\vec{s}'_{22}=\vec{t}_{21}+\vec{t}_{23}=a_2(1,0,1),$$

$$\vec{s}'_{23}=-\vec{t}_{22}=a_2(0,-1,0). \tag{29}$$

The setting of $Pmmn$ in the International Tables[24] (origin choice 2) is obtained by shifting the origin of G with respect to G_1 by $-\frac{1}{2}\vec{t}_{11}+\frac{1}{2}\vec{t}_{13}$, and we obtain the generators of G using the new coordinates defined above, $\{C_{2x}|\frac{1}{2}\vec{s}'_{11}\}$, $\{C_{2y}|\frac{1}{2}\vec{s}'_{12}\}$, $\{I|0\}$. We also obtain these generators from G_2 by shifting the origin of G with respect to G_2 by $\frac{1}{2}\vec{t}_{21}+\frac{1}{4}\vec{t}_{22}$.

Next, we consider atomic displacements along the path from G_1 to G_2. The atoms in a crystal belong to a finite number of sets called Wyckoff positions. Types of Wyckoff positions are labeled (a), (b), (c), etc., in the International Tables. Two different sets of atoms which belong to the same type of Wyckoff position can be brought into each other's positions by a continuous change. Small displacements cannot change the type of Wyckoff positions a set of atoms belongs to without changing the space-group symmetry of the crystal. Therefore, atoms must remain in the same types of Wyckoff positions along the entire path from G_1 to G_2. This means that Wyckoff positions near one end point of the path where G becomes G_1 must be the same type near the other end point where G becomes G_2. This gives us an easy method to tell whether it is possible for atomic positions to evolve from G_1 to G_2 along the path given by the common subgroup G.

However, we must be careful. The type of Wyckoff position can depend on the origin of the space group. For example, in NaCl (structure in G_1), the Na and Cl atoms are at Wyckoff positions *a* and *b*, respectively, if the origin is at a Na atom, and at Wyckoff positions *b* and *a*, respectively, if the origin is at a Cl atom. We therefore consider all possible shifts $\vec{\tau}'$ of the origin of G at the end point near G_2 such that the translational part $\vec{v}_j$ of the operators in G remain the same (to within a lattice vector in T). We must solve the equation

$$\hat{R}_j\vec{\tau}'-\vec{\tau}'=0 \tag{30}$$

for $\vec{\tau}'$ (to within a lattice vector in T) simultaneously for each point operation $\hat{R}_j$ in G. As before, we use the method of Smith normal forms to find solutions. For some space groups, the solutions to this equation depend on a continuously variable parameter; i.e., there are an infinite number of solutions. For example, the origin of space group 75 $P4$ can be anywhere along the *z* axis without affecting the translation part $\vec{v}_j$ of any of the operators in that space group. We deal with these parameters below.

A type of Wyckoff position may have up to three degrees of freedom, including zero degrees of freedom when the atoms are at fixed positions. These degrees of freedom are usually denoted in International Tables by one or more of the symbols x,y,z. We call these "Wyckoff structural parameters." For example, in space group 221 $Pm\bar{3}m$, one of the atoms at Wyckoff position (g) is at x,x,x. This position has one degree of freedom and hence one Wyckoff structural parameter, in this case labeled with *x*.

Sometimes, a Wyckoff position with different values of the structural parameters can describe the same set of atoms. In the above example, suppose that $x=0.214$; i.e., there is an atom at (0.214,0.214,0.214). We see from the International Tables that there is another atom at $\bar{x},\bar{x},\bar{x}$ or $(-0.214,-0.214,-0.214)$. But this position also has the form x,x,x with $x=-0.214$. Therefore, Wyckoff position (g) with either $x=0.214$ or $x=-0.214$ describes the same set of atomic positions. When we try mapping atoms at the two ends of the path from G_1 to G_2, we must consider all possible values of the Wyckoff structural parameters that describe the atomic positions.

Now we are ready to map atoms at one end of the path onto atoms at the other end of the path. At each end of the path we must have the same types of Wyckoff positions. They are only allowed to differ in the values of the Wyckoff structural parameters. We assume that these parameters vary continuously from their values at one end of the path to their values at the other end of the path. If there are any continuously variable parameters in the allowed origin shifts of G as described above, we choose these values at the end point near G_2 to minimize the change in the Wyckoff structural parameters along the path.

Now we have a possible path from G_1 to G_2. Along this path, the lattice parameters change and the Wyckoff structural parameters change. We check one more thing. We look at a structure halfway between the two end points of the path. In this structure, the lattice and Wyckoff parameters are chosen to be halfway between their values at the two end points of the path. We calculate nearest-neighbor atomic distances in this structure. If this is too small, we reject this path. Along this path, the lattice would need to expand to allow atoms to pass by each other, and we assume that such a strain would result in an energy barrier unfavorable for this path.

Let us return once more to the example above. We found two cases for further consideration: (1) $Pmmm$ and (2) $Pmmn$. In both G_1 and G_2, the Na atoms are at Wyckoff position (a) and the Cl atoms are at (b). In case (1), position (a) in G_1 becomes positions (a) and (h) in G, and position (a) in G_2 becomes positions (a) and (d) in G. There is no way that a structure with atoms at (a) and (h) can evolve continuously to a structure with atoms at (a) and (d) without losing the symmetry $Pmmm$ of G. No change in origin will remedy this situation. Therefore, we must reject case (1) as a possible path for the phase transition.

On the other hand, in case (2), we find that in G, the Na atoms are at position (a) and the Cl atoms are at (b) at both ends of the path. Therefore, we consider this case further. Below, we give the structural parameters for G at the two end points of the path from G_1 to G_2.

Lattice parameters:

$$a = 4.84\ \text{Å} \rightarrow 4.21\ \text{Å},$$

$$b = 3.42\ \text{Å} \rightarrow 4.21\ \text{Å},$$

$$c = 3.42\ \text{Å} \rightarrow 2.98\ \text{Å}. \tag{31}$$

Atoms positions:

$$\text{Na:} \quad (\tfrac{1}{4},\tfrac{1}{4},\tfrac{3}{4}) \rightarrow (\tfrac{1}{4},\tfrac{1}{4},1),$$

$$\text{Cl:} \quad (\tfrac{1}{4},\tfrac{3}{4},\tfrac{1}{4}) \rightarrow (\tfrac{1}{4},\tfrac{3}{4},\tfrac{1}{2}), \tag{32}$$

We must check one more thing. In G_1, the nearest-neighbor distance is 2.42 Å, and in G_2 it is 2.58 Å. In the structure at the midpoint between the structures at the two ends of the path, the nearest-neighbor distance is 2.49 Å. It appears that atoms do not approach each other unreasonably close along this path. Therefore, we accept this path as a possible mechanism for the phase transition in NaCl.

III. RESULTS FOR NaCl

We applied the COMSUBS algorithm to the case of the pressure-induced phase transition in NaCl. For the low-pressure structure, $G_1 = Fm\bar{3}m$ with lattice parameter $a_1 = 4.84$ Å. For the high-pressure structure, $G_2 = Pm\bar{3}m$ with lattice parameter $a_2 = 2.98$ Å. We used the following criteria

(1) We considered only subgroups where the length of the generators $\vec{s}_{ij}$ are 6 Å or less.

(2) We considered only subgroups where the principal elements of the strain tensor are less than $1+\epsilon$ and greater than $(1+\epsilon)^{-1}$, where $\epsilon = 0.5$.

(3) The nearest-neighbor distance is 2.42 Å in G_1 and 2.58 Å in G_2. We considered only subgroups where the nearest-neighbor distance in the structure halfway between G_1 and G_2 is greater than 2.00 Å (80% of the average of 2.42 Å and 2.58 Å).

(4) We considered only maximal subgroups. These define the possible mappings of atoms in G_1 onto atoms in G_2. Subgroups of these maximal subgroups do not introduce new mappings. They only alter the path by allowing additional distortions in G along the path. We will show how we consider the nonmaximal subgroups when we discuss the $R\bar{3}m$ path in detail below.

Using these criteria, we obtained 12 subgroups, which we list in Table I. The first entry in the table is the only common subgroup found where there is no change in the size of the primitive unit cell. The next four entries are subgroups where the size of the primitive unit cell is doubled. The last seven entries are subgroups where the size of the primitive unit cell is four times larger. Subgroups with larger primitive unit cells were not found since we limited the length of the generators $\vec{s}_{ij}$.

The mechanism proposed by Buerger[2] is the first entry, $R\bar{3}m$, and the mechanism proposed by Watanabe *et al.*[6] is the fifth entry, $Pmmn$. (In the Appendix, we treat these two mechanisms in more detail, listing the order parameters and associated distortions.)

In order to push this example further, we must calculate energies of the different structures. We used a first-principles calculation SSCAD,[25] which uses density functional theory with local density approximation for the exchange and correlation energies. SSCAD is not very accurate, but it is fast, and we only intend to use it as an illustration of how to proceed further with this problem.

First, we calculated the energy per Na-Cl pair in both the G_1 and G_2 structures at $T=0$ for various values of the lattice parameters a_1 and a_2, respectively. From an analysis of these data, we obtained a pressure-induced phase transition at $P = 9.95$ GPa with lattice parameters $a_1 = 5.18$ Å and $a_2 = 3.16$ Å. Comparing these results with the experimental values ($P = 30$ GPa, $a_1 = 4.84$ Å, and $a_2 = 2.98$ Å), we see that SSCAD is not very accurate. In general, density functional methods do poorly with predicting the pressure at which such phase transitions take place. However, our goal is to

TABLE I. Maximal common subgroups G of the two phases of NaCl, $G_1=Fm\bar{3}m$ and $G_2=Pm\bar{3}m$. G provides a possible path for the transition of NaCl from G_1 to G_2. At each end point of the path ($G\rightarrow G_i$), we give the conventional lattice vectors $\vec{s}_{i1},\vec{s}_{i2},\vec{s}_{i3}$ of G in terms of the conventional lattice vectors of G_i as well as the atomic postions in G (Wyckoff symbols in parentheses). In the last column, an estimate of the free energy barrier $\Delta\Phi_{\rm est}$ is given.

G	$\vec{s}_{12},\vec{s}_{12},\vec{s}_{13}$	$\vec{s}_{21},\vec{s}_{22},\vec{s}_{23}$	Atoms	at G_1	at G_2	$\Delta\Phi_{\rm est}$ (eV)
166 $R\bar{3}m$	$(\frac{1}{2},0,\frac{1}{2}),(0,\frac{1}{2},\bar{\frac{1}{2}}),(\bar{1},1,1)$	$(0,1,1),(\bar{1},\bar{1},0),(1,\bar{1},1)$	Na (a)	0,0,0	0,0,0	0.077
			Cl (b)	0,0,1/2	0,0,1/2	
5 $C2(1)$	$(\frac{1}{2},\bar{1},\bar{\frac{1}{2}}),(\frac{1}{2},0,\frac{1}{2}),(\bar{\frac{1}{2}},\bar{1},\frac{1}{2})$	$(0,1,\bar{1}),(0,1,1),(2,0,0)$	Na (a)	0,0,0	0,1/6,0	0.91
			Na (b)	0,1/2,1/2	0,1/6,1/2	
			Cl (c)	1/4,1/2,3/4	0,2/3,3/4	
5 $C2(2)$	$(\frac{1}{2},\bar{1},\bar{\frac{1}{2}}),(\frac{1}{2},0,\frac{1}{2}),(\bar{\frac{1}{2}},\bar{1},\frac{1}{2})$	$(0,1,\bar{1}),(0,1,1),(2,0,0)$	Na (c)	1/4,1/2,3/4	0,1/3,3/4	0.90
			Cl (a)	0,0,0	$0,-1/6,0$	
			Cl (b)	0,1/2,1/2	0,5/6,1/2	
36 $Cmc2_1$	(0,1,0),(0,0,1),(1,0,0)	$(\bar{1},0,1),(1,0,1),(0,2,0)$	Na (a)	$0,-1/4,0$	0,0,1/8	2.08
			Cl (a)	0,3/4,1/2	0,1/2,3/8	
59 $Pmmn$	$(1,0,0),(0,\frac{1}{2},\bar{\frac{1}{2}}),(0,\frac{1}{2},\frac{1}{2})$	$(1,0,\bar{1}),(1,0,1),(0,\bar{1},0)$	Na (a)	1/4,1/4,3/4	1/4,1/4,1	0.10
			Cl (b)	1/4,3/4,1/4	1/4,3/4,1/2	
13 $P2/c(1)$	$(1,\bar{\frac{1}{2}},\frac{1}{2}),(0,\bar{\frac{1}{2}},\bar{\frac{1}{2}}),(1,\frac{1}{2},\bar{\frac{1}{2}})$	$(0,0,\bar{2}),(\bar{1},\bar{1},0),(\bar{1},1,0)$	Na (g)	3/4,3/4,0	$3/4,3/4,-1/4$	1.17
			Cl (e)	0,3/4,1/4	0,3/4,1/4	
			Cl (f)	1/2,1/4,1/4	1/2,3/4,1/4	
13 $P2/c(2)$	$(1,\bar{\frac{1}{2}},\frac{1}{2}),(0,\bar{\frac{1}{2}},\bar{\frac{1}{2}}),(1,\frac{1}{2},\bar{\frac{1}{2}})$	$(0,0,\bar{2}),(\bar{1},\bar{1},0),(\bar{1},1,0)$	Na (e)	0,1/4,1/4	0,1/4,1/4	1.04
			Na (f)	1/2,3/4,1/4	1/2,1/4,1/4	
			Cl (g)	1/4,3/4,0	1/4,3/4,1/4	
11 $P2_1/m$	$(1,\frac{1}{2},\bar{\frac{1}{2}}),(0,\frac{1}{2},\frac{1}{2}),(1,\bar{\frac{1}{2}},\frac{1}{2})$	$(1,1,1),(1,0,\bar{1}),(0,2,0)$	Na (e)	0,1/4,1/4	1/4,1/4,1/8	2.15
			Na (e)	1/2,1/4,3/4	1/4,1/4,5/8	
			Cl (e)	3/4,1/4,0	3/4,1/4,1/8	
			Cl (e)	1/4,1/4,1/2	$-1/4,1/4,5/8$	
7 Pc	$(1,\frac{1}{2},\bar{\frac{1}{2}}),(0,\frac{1}{2},\frac{1}{2}),(1,\bar{\frac{1}{2}},\frac{1}{2})$	$(1,1,1),(1,0,\bar{1}),(0,2,0)$	Na (a)	$0,-1/4,0$	$-1/8,0,0$	0.92
			Na (a)	1/2,1/4,0	3/8,1/2,1/4	
			Cl (a)	1/4,3/4,1/4	3/8,1,0	
			Cl (a)	3/4,1/4,1/4	7/8,1/2,1/4	
15 $C2/c$	$(1,0,\bar{1}),(1,0,1),(\frac{1}{2},\bar{1},\bar{\frac{1}{2}})$	$(\bar{2},0,0),(0,2,0),(0,0,\bar{2})$	Na (e)	0,3/8,1/4	0,1/4,1/4	0.58
			Na (e)	0,7/8,1/4	0,3/4,1/4	
			Cl (f)	3/4,5/8,1/4	3/4,1/2,1/2	
2 $P\bar{1}$	$(\frac{1}{2},\bar{1},\bar{\frac{1}{2}}),(1,0,0),(0,0,1)$	$(0,2,0),(1,1,1),(1,0,\bar{1})$	Na (i)	3/4,5/8,5/8	7/8,3/4,3/4	0.40
			Na (i)	3/4,1/8,1/8	5/8,1/4,1/4	
			Cl (i)	1/4,3/8,7/8	3/8,1/4,3/4	
			Cl (i)	1/4,7/8,3/8	1/8,3/4,1/4	
45 $Iba2$	$(1,0,0),(0,\bar{2},0),(0,0,\bar{1})$	$(2,0,0),(0,2,0),(0,0,2)$	Na (c)	1/4,3/8,0	1/4,1/2,1/8	1.33
			Cl (c)	1/4,5/8,0	0,3/4,$-1/8$	

calculate the relative heights of energy barriers, and these relative values are not very sensitive to the pressure used.

At the phase transition from G_1 to G_2, the free energy $\Phi=E+PV$ is at a minimum at the two end points of the path. Along the path, the free energy increases and goes through a maximum value. This is the energy barrier between G_1 and G_2. We can obtain a very rough estimate of the height of the barrier by calculating the free energy Φ for the structure halfway between G_1 and G_2.

For example, consider the first entry in Table I (Buerger's mechanism). We calculate that the lattice parameters for $G=R\bar{3}m$ are $a=3.66$ Å and $c=8.97$ Å at G_1 and $a=4.47$ Å and $c=5.47$ Å at G_2. Halfway between, we obtain the structure with $a=4.06$ Å and $c=7.22$ Å for which we calculate the estimated barrier height to be $\Delta\Phi_{\rm est}=0.077$ eV.

As a second example, consider the fifth entry in Table I (the mechanism of Watanabe *et al.*). We calculate that the lattice parameters for $G=Pmmn$ are $a=5.81$ Å and $b=c=3.66$ Å at G_1 and $a=b=4.47$ Å and $c=3.16$ Å at G_2. Halfway between, we obtain the structure with $a=5.14$ Å,

$b=4.06$ Å, and $c=3.41$ Å. However, we note that the relative positions of the atoms also change along the path. At the midpoint, the Na atoms are at 0,0,7/8 and the Cl atoms are at 0,1/2,3/8. We obtain $\Delta\Phi_{est}=0.101$ eV.

We note that these estimates are upper bounds on the barrier height. The path from G_1 to G_2 which passes over the lowest barrier will most likely not be linear in the structural parameters.

A. $R\bar{3}m$

This is the path proposed by Buerger.[2] The $R\bar{3}m$ path from G_1 to G_2 involves only strains. The Na atoms remain at the lattice points, and the Cl atoms remain at the body-centered positions in the rhombohedral unit cells in $R\bar{3}m$. (Note that in Table I, the atomic positions are given with respect to the hexagonal unit cell.) An animation of Buerger's path can be seen on the internet.[26] We show in Fig. 1 the free energy $\Delta\Phi$ (relative to the values at the two end points of the path) as a function of the volume of the primitive unit cell (containing one Na and one Cl atom). The dashed lines show the free energies of the $G_1=Fm\bar{3}m$ and $G_2=Pm\bar{3}m$ structures.

To obtain the free energy of the $R\bar{3}m$ path over the barrier, we vary the value of the lattice parameter c from 8.97 Å to 5.47 Å (the values at the end points G_1 and G_2, respectively). For each value of c, we minimize the free energy with respect to the lattice parameter a, holding the value of c constant. (Note that if we minimized the free energy holding the volume constant, the structure would always relax to $Pm\bar{3}m$ or $Fm\bar{3}m$, the dashed lines in the figure.) We obtain at the top of the barrier a $R\bar{3}m$ structure with $a=4.06$ Å and $c=6.90$ Å and a barrier height equal to 0.070 eV, which is slightly lower than the estimate in Table I.

Next we consider the possibility that the symmetry of the path from G_1 to G_2 may be some subgroup of $R\bar{3}m$. Remember that we included in Table I only the maximal common subgroups of G_1 and G_2. If we can lower the energy barrier by lowering the symmetry of $R\bar{3}m$, then there will also be a corresponding normal mode lattice vibration which will be unstable. Therefore, we look for unstable normal modes in $R\bar{3}m$ at the top of the barrier.

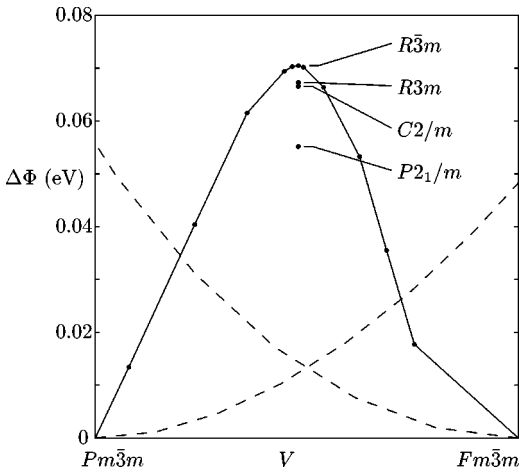

FIG. 1. The relative free energy $\Delta\Phi=\Delta E+PV$ as a function of volume V of the primitive unit cell for the Buerger mechanism in the pressure-induced phase transition in NaCl. The symmetry along the path is $R\bar{3}m$. The dashed lines show the free energy of the two cubic phases, also as a function of V. We also show how the height of the barrier is lowered when we consider paths with less symmetry than $R\bar{3}m$, namely, $R3m$, $C2/m$, and $P2_1/m$.

Using the frozen-phonon method with SSCAD, we calculated the frequencies of the normal modes at each of the **k** points of symmetry in the first Brillouin zone. For $R\bar{3}m$, these are the Γ, F, L, and T points (using the notation of Miller and Love[21]). We found one unstable normal mode at the F point. This mode belongs to the irreducible representation (IR) F_2^- of $R\bar{3}m$. This IR is three dimensional, which means that the mode is threefold degenerate. Any linear combination of the three degenerate modes is unstable. The way in which the unstable mode lowers the symmetry of the crystalline structure depends on the linear combination of

TABLE II. Maximal subgroups of $R\bar{3}m$ which can arise from the F_2^- irreducible representation. At each end point of the path ($G\rightarrow G_i$), we give the conventional lattice vectors $\vec{s}_{i1},\vec{s}_{i2},\vec{s}_{i3}$ of G in terms of the conventional lattice vectors of G_i as well as the atomic postions in G (Wyckoff symbols in parentheses). In the last column, the free energy barrier $\Delta\Phi$ is given.

G	$\vec{s}_{12},\vec{s}_{12},\vec{s}_{13}$	$\vec{s}_{21},\vec{s}_{22},\vec{s}_{23}$	Atoms	at G_1,G_2	$\Delta\Phi$ (eV)
11 $P2_1/m$	$(\frac{1}{2},1,\bar{\frac{1}{2}}),(\bar{\frac{1}{2}},0,\frac{1}{2}),(\bar{\frac{1}{2}},0,\frac{1}{2})$	$(0,\bar{1},1),(0,\bar{1},\bar{1}),(1,0,0)$	Na (e)	1/4,1/4,0	0.05
			Cl (e)	3/4,1/4,1/2	
12 $C2/m$	$(\bar{1},1,0),(\bar{1},\bar{1},0),(0,0,1)$	$(0,\bar{2},0),(2,0,\bar{2}),(1,1,1)$	Na (g)	0,3/4,0	0.066
			Na (i)	3/4,0,1/2	
			Cl (h)	0,1/4,1/2	
			Cl (i)	1/4,0,0	
160 $R3m$	$(\bar{1},0,\bar{1}),(0,\bar{1},1),(\bar{1},1,1)$	$(0,\bar{2},\bar{2}),(2,2,0),(1,\bar{1},1)$	Na (a)	0,0,0	0.067
			Na (b)	$1/6,-1/6,1/3$	
			Cl (a)	0,0,1/2	
			Cl (b)	$-1/6,1/6,1/6$	

these three modes. In this case, there are six possible lower symmetries, all subgroups of $R\bar{3}m$ (called isotropy subgroups; see the Appendix or Stokes and Hatch[27]). Of these six subgroups, three of them are maximal, and we list them in Table II. The other three are subgroups of those listed in Table II and will be automatically considered when we look for unstable normal modes in the maximal subgroups.

We relaxed each of the structures in Table II, always holding one structural parameter constant. For example, consider the $P2_1/m$ structure. There are eight structural parameters: the lattice parameters a,b,c,β and the Wyckoff parameters x,z for each of the two (e) sites. We held the monoclinic angle β constant and relaxed the remaining seven parameters. (If we relaxed all eight parameters, the structure would ''slide down the hill'' and end up at one of the end points, G_1 or G_2.) We obtained

$$\begin{aligned} a &= 5.09 \text{ Å}, \\ b &= 3.46 \text{ Å}, \\ c &= 3.26 \text{ Å}, \\ \beta &= 107.5°, \\ x_{\mathrm{Na}} &= 0.270, \\ z_{\mathrm{Na}} &= -0.107, \\ x_{\mathrm{Cl}} &= 0.744, \\ z_{\mathrm{Na}} &= 0.614. \end{aligned} \tag{33}$$

The resulting free energy is $\Delta\Phi = 0.055$ eV. Repeating this procedure for $C2/m$ and $R3m$, we obtain the free energies shown in the last column of Table II. These three energies are plotted on Fig. 1. As can be seen, the barrier is lowest for the $P2_1/m$ path.

We must also consider the possibility that some subgroup of $P2_1/m$ may provide a path with an even lower barrier. (Remember that we only considered the maximal isotropy subgroups of $R\bar{3}m$.) We look for unstable normal modes in the $P2_1/m$ structure just as we did for $R\bar{3}m$. We calculated the frequencies of the normal modes at each of the **k** points of symmetry in the first Brillouin zone of $P2_1/m$ and found no unstable modes (except for the Γ_1^+ IR which preserves the $P2_1/m$ symmetry and simply represents ''sliding down the hill'' towards G_1 or G_2). We therefore conclude that the lowest barrier for the Buerger mechanism (with our modification) is encountered for the path with $P2_1/m$ symmetry.

B. *Pmmn*

This is the path proposed by Watanabe *et al*. The $Pmmn$ path from G_1 to G_2 involves not only strains but also atomic shuffles. An animation of the path of Watanabe *et al.* can be seen on the internet.[26] There are five structural parameters: the lattice parameters a,b,c and the Wyckoff parameter z for the Na (a) site and for the Cl (b) site. To obtain the free energy along the path from G_1 to G_2, we choose values of the Wyckoff parameter z for the Na (a) site and hold it constant while minimizing the free energy with respect to the remaining four structural parameters. At the top of the barrier, we obtain the $Pmmn$ structure with

$$\begin{aligned} a &= 4.98 \text{ Å}, \\ b &= 4.04 \text{ Å}, \\ c &= 3.31 \text{ Å}, \\ z_{\mathrm{Na}} &= 0.880, \\ z_{\mathrm{Cl}} &= 0.369, \end{aligned} \tag{34}$$

and a free energy $\Delta\Phi = 0.077$ eV. We found no unstable normal modes (except for those associated with the Γ_1^+ IR) and therefore conclude that the height of barrier for the mechanism of Watanabe *et al.* is $\Delta\Phi = 0.077$ eV. We note that this barrier is not as low as the $P2_1/m$ path for our modified Buerger mechanism. However, we recognize that SSCAD is not a very accurate way to calculate energy and that the difference between 0.055 eV and 0.077 eV is not large enough for us to be able to conclude that the Buerger mechanism is energetically more favorable than the mechanism of Watanabe *et al.* (In CsCl there is a temperature-induced phase transition to the NaCl structure at 445 °C. There is evidence from x-ray single-crystal and optical microscope studies that this phase transition takes place via the mechanism of Watanabe *et al*.[6])

There has been some previous work on the mechanistic aspects of a phase transition of this type. Ruff *et al.*[29] concluded that the mechanism of Watanabe *et al.* was favored for RbBr on the basis of isothermal-isobaric molecular dynamics. Nga and Ong,[5] using two different molecular dynamics algorithms, show that the two mechanisms are roughly equivalent in NaCl. Pendás *et al.*[30] carried out a study of the Buerger mechanism in LiCl using an *ab initio* perturbed ion method. Our first-principles calculations are consistent with these findings.

IV. CONCLUSION

We have described and implemented a systematic method called COMSUBS which finds possible mechanisms for a given reconstructive phase transition. Each mechanism describes a path between the two phases. Along this path, the crystalline structure has a definite symmetry which is a common subgroup of the symmetries of the two phases. COMSUBS may be applied to any reconstructive phase transition. We applied COMSUBS to the pressure-induced phase transition in NaCl and found 12 possible paths.

Given the possible paths, there exist a number of methods for determining which one is most energetically favorable. We have demonstrated one such method for the case of the phase transition in NaCl. Using the program SSCAD for first-principles energy calculations, we determined that the path proposed by Buerger and the path proposed by Watanabe *et al.* are both much more energetically favorable than any of the other ten paths found by COMSUBS.

Note added in proof. It has come to our attention that an intermediate phase with the monoclinic $P2_1/m$ symmetry has been observed[31] for a Buerger-like mechanism in the pressure-induced NaCl-CsCl phase transition in the silver halides. Furthermore, recent *ab initio* calculations[32] for AgBr have confirmed the existence of this stable monoclinic intermediate phase.

APPENDIX: ORDER PARAMETERS

In the Landau theory of phase transitions, distortions which accompany a transition are decomposed into parts belonging to different irreducible representations of the parent space group. Order parameters $\vec{\eta}$, which are vectors in representation space, govern the amplitude of these distortions. In the parent phase, the order parameters are zero, and at the transition, the order parameters become nonzero.

In reconstructive phase transitions, either G_1 or G_2 could be considered to be the parent space group, since in either case a distortion reduces the symmetry to the subgroup G. Let us call G_1 the parent space group. When the crystal has the symmetry G_1, the order parameters are zero. At the transition, the order parameters become nonzero, reducing the symmetry to G. As the crystal moves along the path from G_1 to G_2, the amplitudes of the order parameters evolve, generally increasing in magnitude, until they reach particular values. At that point, the symmetry of the crystal increases and becomes G_2.

Distortions associated with a particular order parameter and IR reduce the symmetry of G_1 to some symmetry H which is a subgroup of G_1. The symmetry group H is called an isotropy subgroup of G_1. Each order parameter determines an isotropy subgroup. If the isotropy subgroup H is equal to G, then the order parameter is called a primary order parameter and the associated distortion reduces the symmetry of G_1 all the way to G. Secondary order parameters determine isotropy subgroups H which are supergroups of G. The distortion associated with a secondary order parameter reduces the symmetry of G_1 to some structure which has more symmetry than G.

Let us illustrate this with the pressure-induced phase transition in NaCl discussed in great detail in this paper. In Table III, we list the order parameters for various paths from G_1 to G_2. We obtained these results with the aid of a software package ISOTROPY.[28]

The first entry in Table III is Buerger's $R\bar{3}m$ path. We see that the distortions which occur along the path are strains e. We use a notation $e=(e_1,e_2,e_3,e_4,e_5,e_6)$ which denotes the strain tensor

$$e=\begin{pmatrix} e_1 & e_4 & e_6 \\ e_4 & e_2 & e_5 \\ e_6 & e_5 & e_3 \end{pmatrix}, \tag{A1}$$

which we define so that a vector

$$\vec{r}=\sum_i r_i\hat{e}_i, \tag{A2}$$

which is tied to points in the crystal, becomes, under the action of the strain,

$$\vec{r}\,'=\sum_{i,j} e_{ij}r_j\hat{e}_i. \tag{A3}$$

In the above equations, $\hat{e}_i$ refers to unit vectors of a Cartesian coordinate system. Do not confuse this with the components e_i of the strain.

In the $G_1=Fm\bar{3}m$ structure of NaCl, a general strain can be decomposed into parts which belong to the following IRs (using the notation of Miller and Love[21]):

$$\begin{aligned} &\Gamma_1^+: \quad (a,a,a,0,0,0), \\ &\Gamma_3^+: \quad (a,a,2\bar{a},0,0,0),(\sqrt{3}a,\sqrt{3}\bar{a},0,0,0,0), \\ &\Gamma_5^+: \quad (0,0,0,a,0,0),(0,0,0,0,a,0),(0,0,0,0,0,a). \end{aligned} \tag{A4}$$

We note that Γ_3^+ is a two-dimensional IR. The two strains listed above for Γ_3^+ transform like the two basis functions of Γ_3^+. The order parameter $\vec{\eta}$ associated with that IR is therefore also two dimensional, the two components of $\vec{\eta}$ representing the amplitudes of those two strains. For example, the order parameter $\vec{\eta}=(\eta_1,\eta_2)$ would denote the strain $(\eta_1+\sqrt{3}\eta_2,\eta_1-\sqrt{3}\eta_2,-2\eta_1,0,0,0)$. Similarly, Γ_5^+ is a three-dimensional IR, and the associated order parameter is therefore also three dimensional.

From Table III, we see that the strain along the $R\bar{3}m$ path is decomposed into parts that belong to the IR's, Γ_1^+ and Γ_5^+. The strain along the entire $R\bar{3}m$ path from G_1 to G_2 is characterized by two independent amplitudes η_1 and η_2.

Note that the part of the strain that belongs to Γ_5^+ is a specific combination $\vec{\eta}=(\eta_2,\bar{\eta_2},\eta_2)$ of the three strains listed above for Γ_5^+. The evolution of this part of the strain along the $R\bar{3}m$ path is described by the single amplitude η_2.

At the end of the path, G becomes G_2. We can obtain the symmetric form of the strain tensor at that point using the method of magic strains.[20] We first obtain the matrices B_1 and B_2 as defined in Eq. (3). Then we calculate the transformation matrix $S=B_2B_1^{-1}$ which takes an orthogonal coordinate system from G_1 to G_2. We obtain the symmetric strain tensor e from

$$e=U[U^TS^TSU]^{1/2}U^T, \tag{A5}$$

where U^TS^TSU is diagonal (U contains the eigenvectors of S^TS). When we apply this method to the $R\bar{3}m$ path, we obtain the strain tensor at the end of the path:

$$e=\begin{pmatrix} 0.026 & 0.205 & 0.205 \\ 0.205 & 0.026 & -0.205 \\ 0.205 & -0.205 & 0.026 \end{pmatrix}. \tag{A6}$$

We see from inspection that at G_2 the values of the amplitudes η_1,η_2 are equal to 0.026 and 0.205, respectively. Along the path from G_1 to G_2, the values of η_1,η_2 evolve from zero to 0.026,0.205, respectively.

TABLE III. Order parameters along the possible paths for the phase transition in NaCl. The first three paths [$R\bar{3}m, Fmmn, C2(1)$] are from Table I. The last path ($P2_1/m$) is from Table II. We give the space-group symmetry G along the path, the IR of $Fm\bar{3}m$, the order parameter $\vec{\eta}$ (primary order parameters are indicated with *), the isotropy subgroup H associated with the order parameter, the amplitude η_i of the order parameter when the crystal has reached the $G_2 = Pm\bar{3}m$ symmetry at the end of the path, and the distortions (strains and atomic displacements) which take place. The strains e are given in terms of the six components $e_1, e_2, e_3, e_4, e_5, e_6$, and the atomic displacements of the Na and Cl atoms are given in dimensionless units with respect to the fcc unit cell of $Fm\bar{3}m$.

G	IR	$\vec{\eta}$	H	η_i at G_2	Distortions
166 $R\bar{3}m$	Γ_1^+	(η_1)	225 $Fm\bar{3}m$	0.026	$e=(\eta_1,\eta_1,\eta_1,0,0,0)$
	Γ_5^+	$*(\eta_2,\bar{\eta}_2,\eta_2)$	166 $R\bar{3}m$	0.205	$e=(0,0,0,\eta_2,\bar{\eta}_2,\eta_2)$
59 $Pmmn$	Γ_1^+	(η_1)	225 $Fm\bar{3}m$	-0.010	$e=(\eta_1,\eta_1,\eta_1,0,0,0)$
	Γ_3^+	$(\eta_2,\sqrt{3}\eta_2)$	139 $I4/mmm$	-0.060	$e=(2\eta_2,\bar{\eta}_2,\bar{\eta}_2,0,0,0)$
	Γ_5^+	$(0,\eta_3,0)$	71 $Immm$	-0.180	$e=(0,0,0,0,\eta_3,0)$
	X_5^-	$*(0,0,0,0,0,\eta_4)$	59 $Pmmn$	1/8	Na1$=(0,\eta_4,\eta_4)$, Na2$=(0,\bar{\eta}_4,\bar{\eta}_4)$
	X_5^-	$*(0,0,0,0,0,\eta_5)$	59 $Pmmn$	1/8	Cl1$=(0,\eta_5,\eta_5)$, Cl2$=(0,\bar{\eta}_5,\bar{\eta}_5)$
5 $C2(1)$	Γ_1^+	(η_1)	225 $Fm\bar{3}m$	0.008	$e=(\eta_1,\eta_1,\eta_1,0,0,0)$
	Γ_3^+	$(\eta_2,\sqrt{3}\bar{\eta}_2)$	139 $I4/mmm$	-0.135	$e=(\bar{\eta}_2,2\eta_2,\bar{\eta}_2,0,0,0)$
	Γ_5^+	$(\eta_3,\bar{\eta}_3,\eta_4)$	12 $C2/m$	0.106,0.088	$e=(0,0,0,\eta_3,\bar{\eta}_3,\eta_4)$
	Γ_4^-	$(\eta_5,0,\eta_5)$	44 $Imm2$	$-1/24$	Na1$=(\eta_5,0,\eta_5)$, Na2$=(\eta_5,0,\eta_5)$
	Γ_4^-	$(\eta_6,0,\eta_6)$	44 $Imm2$	1/12	Cl1$=(\eta_6,0,\eta_6)$, Cl2$=(\eta_6,0,\eta_6)$
	L_1^+	$(0,\eta_7,0,0)$	166 $R\bar{3}m$	0	Cl1$=(\bar{\eta}_7,\bar{\eta}_7,\eta_7)$, Cl2$=(\eta_7,\eta_7,\bar{\eta}_7)$
	L_3^+	$*(0,0,(2+\sqrt{3})\eta_8,\bar{\eta}_8,0,0,0,0)$	12 $C2/m$	1/8	Cl1$=(\bar{\eta}_8,2\eta_8,\eta_8)$, Cl2$=(\eta_8,2\bar{\eta}_8,\bar{\eta}_8)$
	L_3^-	$*(0,0,\eta_9,(2+\sqrt{3})\eta_9,0,0,0,0)$	15 $C2/c$	1/8	Na1$=(\eta_9,0,\eta_9)$, Na2$=(\bar{\eta}_9,0,\bar{\eta}_9)$
11 $P2_1/m$	Γ_1^+	(η_1)	225 $Fm\bar{3}m$	0.026	$e=(\eta_1,\eta_1,\eta_1,0,0,0)$
	Γ_3^+	$(\eta_2,\sqrt{3}\bar{\eta}_2)$	139 $I4/mmm$	0	$e=(\bar{\eta}_2,2\eta_2,\bar{\eta}_2,0,0,0)$
	Γ_5^+	$(\eta_3,\bar{\eta}_3,\eta_4)$	12 $C2/m$	-0.205,0.205	$e=(0,0,0,\eta_3,\bar{\eta}_3,\eta_4)$
	X_3^-	$*(\eta_5,0,0)$	129 $P4/nmm$	0	Na1$=(0,\eta_5,0)$, Na2$=(0,\bar{\eta}_5,0)$
	X_3^-	$*(\eta_6,0,0)$	129 $P4/nmm$	0	Cl1$=(0,\eta_6,0)$, Cl2$=(0,\bar{\eta}_6,0)$
	X_5^-	$*(\eta_7,0,0,0,0,0)$	59 $Pmmn$	0	Na1$=(\eta_7,0,\bar{\eta}_7)$, Na2$=(\bar{\eta}_7,0,\eta_7)$
	X_5^-	$*(\eta_8,0,0,0,0,0)$	59 $Pmmn$	0	Cl1$=(\eta_8,0,\bar{\eta}_8)$, Cl2$=(\bar{\eta}_8,0,\eta_8)$

In Table III we list the isotropy subgroups H for each order parameter. We note that for the $R\bar{3}m$ path the isotropy subgroup H associated with the order parameter for Γ_5^+ is $R\bar{3}m$. The strain with amplitude η_2 reduces the symmetry of $Fm\bar{3}m$ all the way to $R\bar{3}m$. This is a primary order parameter.

The isotropy subgroup associated with the order parameter for Γ_1^+ is $Fm\bar{3}m$ which is the same as G_1. The diagonal strain tensor with amplitude η_1 does not reduce the symmetry of G_1 at all. It simply causes a change in volume. It is a secondary order parameter.

The next entry in Table III is the $Pmmn$ path of Watanabe *et al*. Here we see that in addition to strains, atomic displacements are also listed as distortions. They belong to the six-dimensional IR X_5^-. This IR is listed twice in the table since the displacements of the Na and Cl are independent of each other and are therefore governed by two independent order parameters, each belonging to the same IR X_5^-.

From Table I, we see that along the path from G_1 to G_2, the Na atom moves from (1/4,1/4,3/4) to (1/4,1/4,1). The displacement is thus equal to (0,0,1/4) in terms of the unit cell of $Pmmn$ and equal to (0,1/8,1/8) in terms of the unit cell of $G_1 = Fm\bar{3}m$. This is consistent with Table III, where the displacement of this atom (denoted by Na1) is given by $(0,\eta_4,\eta_4)$. The value of η_4 varies from zero to 1/8 as the crystal evolves from G_1 to G_2.

Na2 is the other Na atom in the unit cell belonging to the Wyckoff (a) position. It moves from (3/4,3/4,1/4) to (3/4, 3/4,0) along the path, its displacement being in a direction opposite to that of Na1.

There are two primary order parameters. Both the Na and the Cl displacements reduce the symmetry of G_1 all the way to $Pmmn$.

The $C2$ (1) path in Table III is an example of a more complex situation. (This path is the second entry in Table I.) There are nine structural parameters, five of them strains and four of them atomic displacements. We note that two of the IRs, L_3^+ and L_3^-, are eight dimensional.

The order parameter associated with Γ_5^+ has two independent amplitudes η_3 and η_4. At the end of the path at G_2, the values of these two amplitudes become 0.106 and 0.088, respectively.

From Table I we see that the displacement of Na1 is equal to $(0,1/6,0)-(0,0,0)=(0,1/6,0)$ in terms of the unit cell of $C2$ and equal to $(1/12,0,1/12)$ in terms of the unit cell of $G_1=Fm\bar{3}m$. Similarly, the displacement of Na2 is equal to $(0,1/6,1/2)-(0,1/2,1/2)=(0,-1/3,0)$ in terms of the unit cell of $C2$ and equal to $(-1/6,0,-1/6)$ in terms of the unit cell of $G_1=Fm\bar{3}m$. This is consistent with Table III, where the displacement of Na1 is equal to $(\eta_5+\eta_9,0,\eta_5+\eta_9)$ and the displacement of Na2 is equal to $(\eta_5-\eta_9,0,\eta_5-\eta_9)$. At G_2, the values $\eta_5=-1/24$ and $\eta_9=1/8$ give us net displacements of $(1/12,0,1/12)$ and $(-1/6,0,-1/6)$ for Na1 and Na2, respectively.

We note in Table III that for the $C2$ path none of the isotropy subgroups are $C2$. None of these distortions alone can reduce the symmetry of G_1 all the way to $C2$. However, the intersection of all of the isotropy subgroups is $C2$, so the combined effect of all of the distortions is to reduce the symmetry to $C2$. In this case, there can be no single order parameter. At least two of the order parameters must be ''coupled'' so that they become nonzero together. In this case, the intersection of $C2/m$ and $C2/c$ is $C2$, so the order parameters associated with L_3^+ and L_3^- are a set of coupled primary order parameters.

The final entry in Table III is the $P2_1/m$ path which is the distorted $R\bar{3}m$ path in Table II with the lowest-energy barrier (according to our calculations). (Do not confuse this with the $P2_1/m$ path in Table I which describes an entirely different atomic mapping.) The distortion at the end point G_2 is identical to that of the $R\bar{3}m$ path. The net atomic displacements are all zero, and the net Γ_3^+ strain, which does not appear in $R\bar{3}m$, is zero. However, along the path, the atomic displacements and the Γ_3^+ strain take on nonzero values. Along the path, they evolve from zero through some nonzero values and then back to zero again at the end of the path. Also note that the Γ_5^+ strain is broken into two independent parts described by two parameters.

Here again we have a case where there is no single primary order parameter. The order parameters associated with X_3^- and X_5^- are a set of coupled primary order parameters.

[1] J.M. Reico, A.M. Pendas, E. Francisco, M. Flores, and V. Luana, Phys. Rev. B **48**, 5891 (1993).

[2] M. Buerger, in *Phase Transformations in Solids*, edited by R. Smoluchwski, J.E. Mayers, and W.A. Weyl (Wiley, New York, 1948), pp. 183–211.

[3] H. Sowa, Acta Crystallogr., Sect. A: Found. Crystallogr. **56**, 288 (2000).

[4] G.S. Nunes, P.B. Allen, and J.L. Martins, Phys. Rev. B **57**, 5098 (1998).

[5] Y.A. Nga and C.K. Ong, Phys. Rev. B **46**, 10 547 (1992).

[6] M. Watanabe, M. Tokonami, and N. Morimoto, Acta Crystallogr., Sect. A: Cryst. Phys., Diffr., Theor. Gen. Crystallogr. **33**, 284 (1977).

[7] J.D. Althoff, P.B. Allen, R.M. Wentzcovitch, and J.A. Moriarty, Phys. Rev. B **48**, 13 253 (1993).

[8] J.C. Jamieson, Science **140**, 72 (1963).

[9] V.A. Zilbershteyn, N.P. Chistotina, A.A. Zarov, N.S. Grishina, and E. I Estrin, Fiz. Met. Metalloved. **39**, 445 (1975).

[10] Y.K. Vohra, S.K. Sikka, S.N. Vaidya, and R. Chidambaram, J. Phys. Chem. Solids **38**, 1293 (1977).

[11] H. Xia, G. Parthasarathy, H. Luo, Y.K. Vohra, and A.L. Ruoff, Phys. Rev. B **42**, 6736 (1990).

[12] G.T. Gray, C.E. Morris, and A.C. Lawson, in *Titanium '92 Science and Technology*, edited by F.H. Froes and I. Caplan (Minerals Metals and Materials Society, Warrendale, PA, 1993).

[13] S. Limpijumnong and W.R.L. Lambrecht, Phys. Rev. Lett. **86**, 91 (2000).

[14] J. Xie, S.P. Chen, J.S. Tse, D.D. Klug, S. Li, K. Uehara, and L.G. Wang, Phys. Rev. B **62**, 3624 (2000).

[15] D.A. Young, *Phase Diagrams of the Elements* (University of California Press, Berkeley, 1991).

[16] L. Liu and W.A. Basset, *Elements, Oxides, Silicates* (Oxford University Press, New York, 1986).

[17] D.M. Hatch, T. Lookman, A. Saxena, and H.T. Stokes, Phys. Rev. B **64**, 060104 (2001).

[18] H. Shoji, Z. Kristallogr. **77**, 381 (1931).

[19] B.G. Hyde and M. O'Keefe, in *Phase Transitions*, edited by L.E. Cross (Pergamon Press, Oxford, 1973), pp. 345–349.

[20] E. Kaxiras and L.L. Boyer, Phys. Rev. B **50**, 1535 (1994).

[21] S.C. Miller and W.F. Love, *Tables of Irreducible Representations of Space Groups and Co-Representations of Magnetic Space Groups* (Pruett, Boulder, 1967).

[22] R.W. Grosse-Kunstleve, Acta Crystallogr., Sect. A: Cryst. Phys., Diffr., Theor. Gen. Crystallogr. **55**, 383 (1999); B. Eick, F. Gahlei, and W. Nickel, *ibid.* **53**, 467 (1997).

[23] D.M. Hatch and H.T. Stokes, Phys. Rev. B **31**, 2908 (1985).

[24] *International Tables for Crystallography*, edited by T. Hahn (Reidel, Boston, 1983), Vol. A.

[25] H.T. Stokes, L.L. Boyer, and M.J. Mehl, Phys. Rev. B **54**, 7729 (1996).

[26] H.T. Stokes and D.M. Hatch, animations of pressure-induced phase transitions in NaCl, www.physics.byu.edu/~stokesh/nacl/

[27] H.T. Stokes and D.M. Hatch, *Isotropy Subgroups of the 230 Crystallographic Space Groups* (World Scientific, Singapore, 1988).

[28] H.T. Stokes and D.M. Hatch (unpublished). ISOTROPY software and documentation are available over the internet at www.physics.byu.edu/~stokesh/isotropy.html. Case study 3 in the tutorial shows specifically how ISOTROPY was used to obtain the decomposition of distortions into IR's given in Table III of this paper.

[29] I. Ruff, A. Baranyai, E. Spohr, and K. Heinzinger, J. Chem. Phys. **91**, 3148 (1989).

[30] A.M. Pendás, V. Luana, J.M. Reico, M. Flórez, E. Francisco, M.A. Blanco, and L.N. Kantorovich, Phys. Rev. B **49**, 3066 (1994).

[31] S. Hull and D.A. Keen, Phys. Rev. B **59**, 750 (1999).

[32] P.T. Jochym and K. Parlinski, Phys. Rev. B **65**, 024106 (2001).